Enhanced Catalytic Activity of Pt Nanomaterials: From Monodisperse Nanoparticles to Self-Organized Nanoparticle-Linked Nanowires

ARTICLE *in* THE JOURNAL OF PHYSICAL CHEMISTRY C · MARCH 2010

Impact Factor: 4.77 · DOI: 10.1021/jp910864w

Enhanced Catalytic Activity of Pt Nanomaterials: From Monodisperse Nanoparticles to Self-Organized Nanoparticle-Linked Nanowires

Gaowu W. Qin,*,† Wenli Pei,† Xiumei Ma,‡ Xiaoning Xu,† Yuping Ren,† Wei Sun,*,‡ and Liang Zuo†

Key Laboratory for Anisotropy and Texture of Materials (Ministry of Education), Northeastern University, Shenyang 110004, China, and Institute of Microstructure & Properties of Advanced Materials, Beijing University of Technology, Beijing 100022, China

Received: November 16, 2009; Revised Manuscript Received: March 17, 2010

The factors affecting the catalytic activity (CA) of monodisperse nanoparticles (NPs), including size, crystallinity, shape, and high indexed facets, have been well-studied these past years; here, we report that the CA is significantly increased when monodisperse Pt near-spherical NPs are cross-linked into Pt nanowires (NWs) using two model catalytic reactions, reduction of either nitrophenol or potassium ferricyanide. In this work, monodisperse Pt NPs or NWs were prepared by using glucose as a surfactant and sodium borohydride as a reducing agent in aqueous solution at room temperature. Monodisperse Pt NPs or Pt NWs can be obtained by simply controlling the molar ratio, R, of the sodium borohydride to the platinum salt, $[NaBH_4]/[Pt^{4+}]$. Different types of Pt NP or NW colloids were used as catalysts in the catalytic reactions above. The results showed that the normalized rate constants of the catalytic reactions increase mildly with increasing particle size for the monodisperse Pt NPs, but they drastically increase for the Pt NWs with a similar mean size as compared with the monodisperse Pt NP colloids. It is thus expected that the large abundance of grain boundaries, generated when NPs are linearly linked into NWs, may be responsible for this enhanced catalytic activity.

1. Introduction

Nanocatalysis has played a major role in petrochemical production and fine chemicals synthesis as well as environmental protection and remediation. Many conventional catalysts are usually based on fine nanoparticles (NPs) with an average size from 1 to 20 nm, such as Pt/C or Rh/Al_2O_3.[1,2] The catalytic activity (CA) is thus strongly dependent on active sites on the catalyst surface, which are usually related to the specific surface area, surface structure, and edges of the catalysts. Because the specific surface area and the number of exposed active sites for a given volume of catalyst increase with a reduction in the catalyst size, much effort has been devoted so far to dispersing and stabilizing catalysts of small clusters or nanosized particles to improve catalytic performance.[1,3]

However, the nature of catalysis in most cases is not yet well-understood, although many catalysts have been developed for some 10−50 years. There should be many other factors besides the size effect addressed to clarify the CA. These past years, Narayanan et al. demonstrated a series of pioneering work that the CA is strongly dependent on the shape of Pt NPs, where tetrahedral Pt NPs have a higher CA than either cubic or spherical NPs with similar sizes.[4] Hermanek et al. reported that there is a competition between the specific surface area and the crystallinity of the Fe_2O_3 catalyst in the decomposition reaction of hydrogen peroxide.[5] More recently, Tian et al. found that tetrahexahedral Pt NPs with high index facets, that is, rich in active valency unsaturated atoms, are also catalytically very active.[6]

This year, Lim et al. demonstrated that Pd-core/Pt-shell nanodendrites are about two times more active based on equivalent Pt mass for the oxygen reduction reaction than the state-of-the-art Pt/C catalyst, and the improvement of the CA is considered to be due to high specific area and particularly more active sites on the Pt surface.[7] Their work suggests an important issue to control the morphology of Pt nanostructures and thus to improve the CA of Pt nanomaterials. Herein, we report that the CA of the Pt catalyst is significantly enhanced when monodisperse Pt NPs change into nanoparticle-linked nanowires (NWs) with the similar mean sizes using two model reactions, the catalytic reduction of either nitrophenol or ferricyanide ions. The specific surface area is decreased with integration of NPs into NWs, but the CA is enhanced obviously. A new catalysis mechanism based on grain boundary defects is thus proposed and discussed in this work.

2. Experimental Section

2.1. Preparation of Pt Nanoparticles and Particle-Linked Nanowires. All reagents were purchased from Sinopharm Chemical reagent Co. Ltd., were reagent grade, and were used without any further purification.

In a typical preparation, 0.2 mL of 0.05 M H_2PtCl_6 solution was added to 50 mL of 0.03 M aqueous glucose solution (pure water of 18.2 MΩ·cm was used). A proper amount of 0.1 M NaOH solution was added dropwise to adjust the pH to 9.1. The solution was stirred for 20 min, and then a desired volume between 0.4 and 5 mL of 0.05 M aqueous $NaBH_4$ solution was added to the system. The formation of either Pt nanoparticles or nanowires depends on the molar ratio, R, of $[NaBH_4]/[Pt^{4+}]$. The detailed description is in the main text. The TEM observation of the Pt NPs or NWs prepared above and their mean size

* To whom correspondence should be addressed. Tel: +86-24-83683772. Fax: +86-24-83686455. E-mail: qingw@smm.neu.edu.cn (G.W.Q.), weisun@bjut.edu.cn (W.S.).
† Northeastern University.
‡ Beijing University of Technology.

10.1021/jp910864w
Published on Web 03/31/2010

distributions are shown in the Supporting Information (Figure S1), taken with a JEOL JEM-2100F transmission electron microscope.

2.2. Catalytic Reduction of Nitrophenol. The catalytic reduction of nitrophenol was studied as follows. In a standard 1 cm quartz photospectroscopic cell, 1.5 mL of 0.1 mM nitrophenol aqueous solution and 1.0 mL of 0.05 M $NaBH_4$ were first mixed. A 0.5 mL portion of Pt nanowire or nanoparticle solution, prepared above and kept at room temperature for 20 h, was added to the cell and mixed well. A decrease in the intensity of the peak of nitrophenol at 400 nm and a simultaneous increase in the intensity of the peaks of aminophenol at both 230 and 300 nm were observed (as shown in Figure S2, Supporting Information). The absorption spectra were recorded every several minutes in the range of 200−600 nm at room temperature on a UV−vis spectrometer (Perkin-Elmer Lambda 750S). For comparison, a blank glucose solution (0.03 M) was added to the cell, and the reaction dynamics is also recorded in Figure S3 (Supporting Information).

2.3. Catalytic Reduction of Potassium Ferricyanide. For the catalytic reduction of potassium ferricyanide, 0.4 mL of 0.01 M potassium ferricyanide, 0.4 mL of 0.1 M sodium thiosulfate aqueous solution, and 2.0 mL of Pt nanoparticle or nanowire colloids, prepared above and kept at room temperature for 20 h, were mixed in the cell. The reaction dynamics was recorded by in situ UV−vis photospectroscopy at room temperature, as shown in Figure S4 (Supporting Information). For comparison, 2.0 mL of blank glucose solution (or 1.5 mL of 0.03 M glucose and 0.5 mL of 0.05 M $NaBH_4$) was added into the cell, and the results showed that there was no effect of glucose and/or $NaBH_4$ on the electron-transfer reaction between the potassium ferricyanide and sodium thiosulfate, as shown in Figure S5 (Supporting Information).

3. Results and Discussion

In this work, we modified the previous preparation method[8] to get Pt nanoparticle-linked NWs using glucose as a surfactant and sodium borohydride as a reducing agent in aqueous solution at room temperature. Monodisperse Pt NPs or Pt NWs can be obtained by simply controlling the molar ratio, R, of the sodium borohydride to the platinum salt, $[NaBH_4]/[Pt^{4+}]$. When R is 2, the solution immediately changes color to light brown from light yellow and further changed to deep brown in 1 h, then finally to gray in about 20 h. The gray color of the solution is stable for more than 2 weeks at room temperature without any sedimentation. It is found that the Pt NPs form at the beginning and then undergo a linear self-organization into stable Pt particle-linked NWs (mean size = 5.7 ± 1.3 nm) with time, as shown in Figure 1a,b. In this case, a large abundance of grain boundaries (Figure 1b) generates between the adjacent near-spherical NPs. It is different from our previous Pt chain-like NWs prepared at a lower pH environment, where each NP is isolated but with linear arrays induced by the capping agent of the glucose.[8] The surface of near-spherical NPs is generally composed of (111) and (200) planes (Figure 1b), which is similar as that observed by Narayanan et al., who prepared the near-spherical Pt NPs by another method.[4] When R is 10, stable monodisperse Pt NPs with a size of 5.0 ± 0.9 nm are obtained. When the mole ratio increases further to 25, a stable colloid of monodisperse Pt NPs with a particle size of 3.7 ± 0.6 nm is obtained (Figure 1c). The size distribution of the Pt NPs is shown in Figure S1 (Supporting Information). Electron diffractions (Figure S1, Supporting Information) indicate that both the Pt NWs and the NPs are nanocrystals.

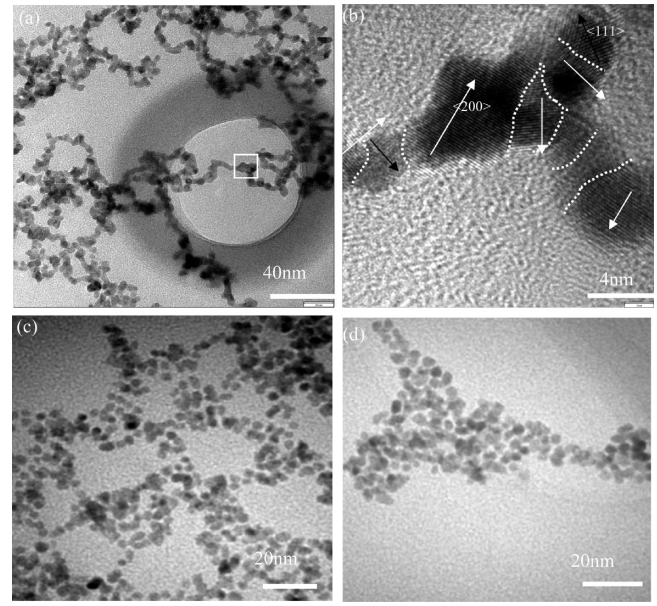

Figure 1. TEM images of Pt NWs and NPs with different R values after a preparation of 20 h. (a) $R = 2$, NWs, 5.7 ± 1.3 nm. (b) HRTEM in the square area of (a); dotted lines are grain boundaries in the Pt NWs. White arrows mean ≃ orientation, black arrows, κ. (c) $R = 10$, NPs, 5.0 ± 0.9 nm. (d) $R = 25$, NPs, 3.7 ± 0.6 nm.

We used these three types of the Pt nanograde catalysts obtained above after a preparation of 20 h to study the competition between the size effect and grain boundary effect on the CA. The procedures to perform the catalysis reactions were the same as those in the literature.[9,10] Two typical reactions were used to determine the CA of the Pt nanomaterials, reduction of nitrophenol by sodium borohydride ($NaBH_4$) and reduction of potassium ferricyanide by sodium thiosulfate. Figure 2a shows representative UV−vis spectra evolution of the reduction of nitrophenol by the Pt NW colloid (0.5 mL) prepared above. A similar spectral pattern was also obtained for the Pt NPs (see the Supporting Information, Figure S2). After the $NaBH_4$ was added into the nitrophenol solution, in the absence of any catalysts, the peak assigned to nitrophenol absorption at ∼400 nm remains unaltered. Addition of 0.5 mL of the Pt nanomaterials made above to the solution (nitrophenol plus $NaBH_4$) resulted in a color fading and eventual bleaching of the nitrophenol solution. The reduction reaction is further proved by the disappearance of the 400 nm peak with the concomitant appearance of new peaks at ∼230 and ∼300 nm. These peaks are assigned to the aminophenol.[9,10] To exclude the effect of Pt nanomaterials on the determined UV−vis spectra, the UV−vis spectrum of either Pt nanoparticle or nanowire solution was determined and it was found that there are no characteristic peaks in the determined band (250−600 nm), as shown in the Supporting Information (Figure S2d).

Strictly speaking, UV/vis spectroscopy is an extinction spectroscopy, and in this region of the electromagnetic spectrum, molecules undergo electronic transitions from the ground state to the excited state. For the transparent liquid samples, because the reflection and scattering are low, thus absorption is used to characterize the concentration of a specific molecule in a given solution. Because the concentration of the borohydride ion is much higher than that of nitrophenol and the catalysts, pseudo-first-order kinetics of the nitrophenol reduction can be used to evaluate the reaction rate and catalytic activity (CA).[10] A good linear correlation of $\ln(A)$ versus time is obtained for all the systems studied (Figure 2b), where A is the absolute absorbance

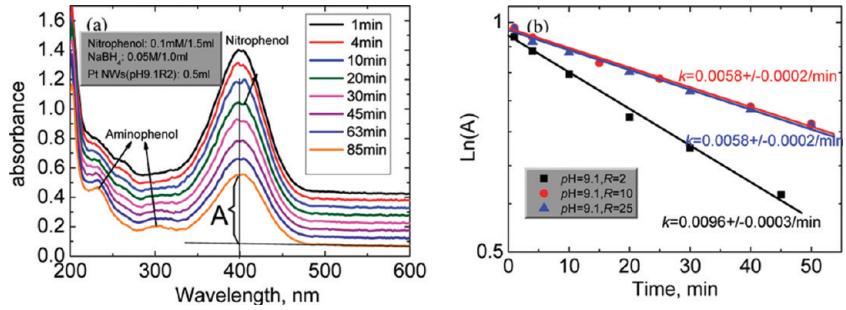

Figure 2. Catalytic reduction of nitrophenol with $NaBH_4$ by using various Pt nanomaterials: (a) typical time-dependent UV−vis spectra on the reduction of nitrophenol by Pt nanowires (pH = 9.1, R = 2), where all the UV/vis spectroscopy patterns were offset, and (b) plots of ln(A) vs time for the reaction by various Pt nanomaterials.

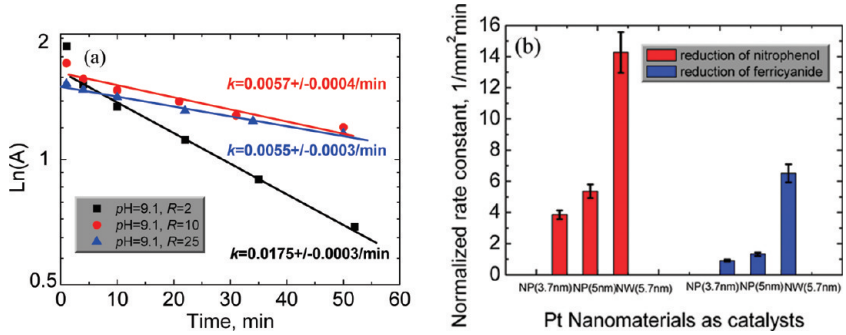

Figure 3. Plots of ln(A) vs time for the catalytic reduction of potassium ferricyanide by Pt nanomaterials prepared under various conditions (a) and the normalized rate constants of the two catalytic reactions using monodisperse Pt NPs or linearly particle-linked NWs (b).

of the characteristic peak at a catalytic reaction time t corrected by the background absorbance, as shown in Figure 2a. The values of the pseudo-first-order rate constants (k) calculated from these plots are given in Figure 2b. It is found that the reaction rate constants are the same for the Pt NPs catalysts with different mean sizes, whereas it is ~65% higher for the Pt NW catalysts. Considering the density of Pt nanomaterials (NWs or NPs) in the prepared solution is a little different by different R values, we change the apparent rate constants into ones in per weight of Pt nanomaterials. The rate constant is 0.50 ± 0.02/mg·min for the Pt NW catalyst (R = 2, 0.01928 mg of Pt for 0.5 mL), 0.31 ± 0.01/mg·min for the Pt NPs (R = 10, 0.01869 mg of Pt for 0.5 mL), and 0.33 ± 0.01/mg·min for the Pt NPs (R = 25, 0.01767 mg of Pt for 0.5 mL). As it is shown, the rate constant is similar for the Pt NP catalyst, whereas it is still ~60% higher for the Pt NW catalyst. Considering different particle sizes and size distributions of these three Pt nanomaterials used here (see the Supporting Information, Figure S1), we further normalized the rate constant by per surface area of either Pt NPs or NWs, as shown in Figure 3b. Because the Pt mass used for the catalytic reaction is known for either NPs or NWs and their size and size distribution can be obtained by TEM observation, the surface area of either NPs or NWs at a given mass or volume (0.5 mL of Pt for the nitrophenol reduction reaction) can thus be calculated, which is (6.73 ± 0.61) × 10^{-4} mm^2, (1.08 ± 0.09) × 10^{-3} mm^2, and (1.51 ± 0.11) × 10^{-3} mm^2 for the case of R = 2, 10, and 25, respectively. Please see the Supporting Information for the details. With increasing particle size, the normalized rate constant mildly increases. This finding is in good agreement with that observed by El-Sayed's group[4] and Sharma et al.;[11] however, the normalized rate constant in this study is increased by ~160% from monodisperse Pt NPs (5.0 nm) to NWs (5.7 nm), as shown in Figure 3b. This suggests that the CA of the Pt NWs is much greater than those of Pt NPs with a similar mean size.

To further verify the effect of Pt NWs on the CA, we conducted another catalytic reduction of potassium ferricyanide using the Pt NP or NW colloids prepared above. This reduction is a typical electron-transfer reaction between the potassium ferricyanide and sodium thiosulfate, which usually reacts slowly at the absence of any catalysts[12] but is accelerated by nanograde Pt catalysts,[4] particularly by the Pt particle-linked NWs in this work. The reduction dynamics of potassium ferricyanide catalyzed by Pt NWs or various NP colloids are shown in Figure S4 (Supporting Information). Figure 3a shows that the apparent rate constant of the reaction for Pt NW catalysts is about 3 folds that of Pt NP catalysts in this catalytic reduction of potassium ferricyanide. By the same token, if the apparent rate constant is changed into one per weight, it is 0.227 ± 0.004/mg·min for the Pt NW catalyst (R = 2, 0.07711 mg of Pt for 2.0 mL), 0.076 ± 0.005/mg·min for the Pt NPs (R = 10, 0.07475 mg of Pt for 2.0 mL), and 0.078 ± 0.004/mg·min for the Pt NPs (R = 25, 0.07069 mg Pt for 2.0 mL). If the rate constant per surface area is considered, the normalized rate constant of Pt NWs (5.7 nm, 6.51 ± 0.58/mm^2 min) is either more than 4 folds that of Pt NPs (5.0 nm, 1.32 ± 0.11/mm^2 min) or more than 7 folds that of Pt NPs (3.7 nm, 0.91 ± 0.07/mm^2 min), as shown in Figure 3b.

On comparison of the Pt NP (5.0 nm) and NW (5.7 nm) colloids, the NPs in either monodisperse NPs or NW solution are near-spherical, and TEM analysis shows that they are stable before and after the catalytic reactions with little change in their shape. It is reasonable because the near-spherical NPs have the lowest surface energy, which has been experimentally confirmed by El-Sayed's group.[4] For the two types of monodisperse Pt NPs with different mean sizes, only a slighter increase of the normalized rate constants is observed in both catalytic reactions for the larger size Pt NPs. However, our results show that the CA is greatly enhanced by the Pt NWs. Considering the difference between Pt NWs and NPs, the size effect plays a

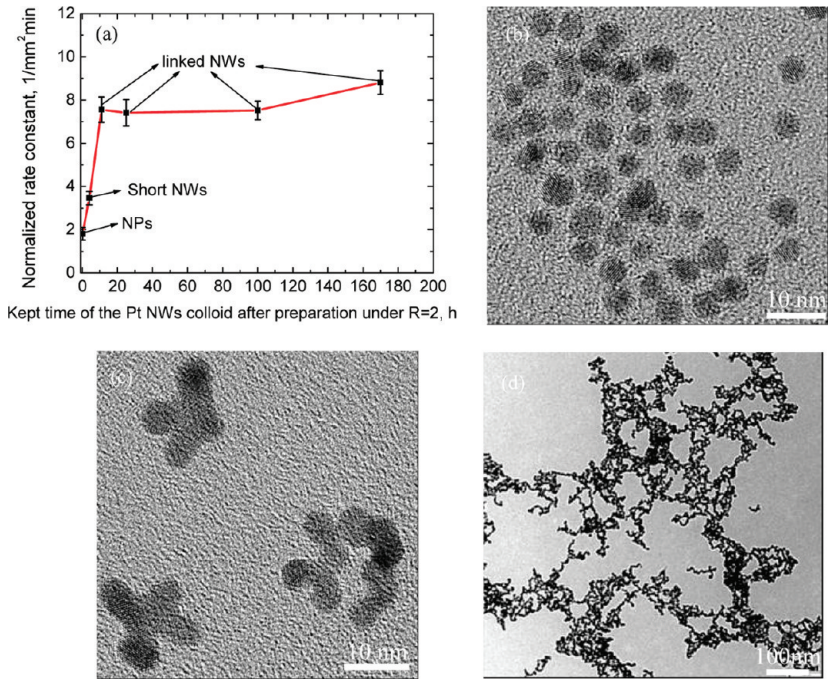

Figure 4. Rate constant of the catalytic reduction of potassium ferricyanide vs kept time of the Pt nanomaterials prepared at $R = 2$ and kept at room temperature for different times (a), where they underwent monodisperse Pt NPs (b) (10 min after preparation), then short NWs formed (c) (3.5 h after preparation), and finally NWs cross-linked (d) (25 h after preparation).

minor role in the catalytic activity, at least in the size range of 3−6 nm in this study. Instead, the grain boundary, generated by linking NPs to particle-welded NWs, may be responsible for this significant increase of the CA for Pt NWs.

To clarify the effect of glucose and $NaBH_4$ on the catalytic reactions, for comparison, we carried out a clean glucose solution test without any Pt NW or NP colloids in the reduction of nitrophenol by $NaBH_4$; there is little difference in the UV−vis spectra within 20 min, as shown in Figure S3 (Supporting Information). Similarly, if the glucose and $NaBH_4$ solutions were used instead of the Pt colloids in the reduction of potassium ferricyanide, the reaction was hard to occur (Figure S5, Supporting Information). Obviously, the glucose and/or $NaBH_4$ themselves are hard to affect the CA without the Pt catalyst. But it is worthy to note that the glucose is effective as a capping agent to stabilize either Pt NPs or NWs in aqueous solution, which is important for the two catalytic reactions.

To further confirm the effect of grain boundary on the CA, we conducted a series of catalytic reductions of ferricyanide ions using the Pt nanomaterials prepared at $R = 2$ in different times, where they underwent NPs initially, then short NWs formed, and NWs cross-linked finally. The rate constant changes with the duration time of the Pt NWs after they are prepared at room temperature, as shown in Figure S6 (Supporting Information). The normalized rate constant per surface area increases correspondingly and then approaches a stable value when these Pt NPs are linearly cross-linked after a preparation of ~10 h, as shown in Figure 4. In this dynamics experiment, the normalized rate constant for Pt cross-linked NWs after a preparation of 25 h is $\sim 7.41 \pm 0.61/\text{mm}^2$ min (Figure 4a), which is consistent with the data of $\sim 6.51 \pm 0.58/\text{mm}^2$ min (Figure 3b) in a separate experiment above. It indicates that the results are well-reproducible. These clearly proved that the Pt NWs, which contain a large amount of grain boundaries, have much greater catalytic activity than the monodisperse Pt NPs for a similar size and size distribution.

From the results of the two catalytic reactions, it is found that the CA increases mildly with increasing particle size for the monodisperse NP colloids; however, the CA increases drastically when the monodisperse NPs are linearly linked into NWs. The normalized rate constant of the Pt NWs (5.7 nm) is about 3 folds that of the monodisperse Pt NPs (5.0 nm) in the reduction of nitrophenol and more than 4 folds in the reduction of ferricyanide ions (Figure 3b). In other words, the particle-linked Pt NWs, which contain a large amount of grain boundaries, have a much higher CA than both Pt NPs catalysts for a given mean size of nanoparticles. Therefore, this enhanced CA could be expected to be due to the presence of the grain boundaries in Pt NWs rather than the size effect if we consider their similar particle sizes and little change in their shape before and after the catalytic reactions. The grain boundary density is about 1.8×10^5/mm for the Pt NWs in this study. Grain boundary is a planar defect in polycrystalline materials with a width of 0.5−1.0 nm and can be considered as a linear defect with 0.5−1.0 nm in width in catalytic reactions when they are exposed to the outer surface of the NWs, which may be responsible for this enhanced CA. However, the mechanism of how the grain boundaries of NWs act as catalytic active sites remains unknown, such as how they affect the absorption/desorption of catalyzed molecules in the solution and the efficiency of breaking the molecular binding of either catalyzed chemicals or their complexes. On the other hand, zero valence Pt nanomaterial itself experiences a cycle processing of oxidization and reduction during the catalytic reactions, and the questions of how the surrounding environment for either Pt NPs or NWs in aqueous solution, such surfactants, pH, and the presence of other ions, etc., affects the catalytic behaviors of Pt NPs and NWs need to be systematically studied in future work to clarify the difference in catalytic activity. However, the evidence is clear that the Pt particle-linked NWs have higher catalytic activity in the two model catalytic reactions than Pt monodisperse NPs.

From the results above, if the grain boundary density in the Pt NWs is a key factor to govern the CA, then how to control monodisperse Pt NPs into 1D NP-linked NWs in three dimensions in the aqueous solution rather than normal aggregation is

becoming an important issue. In our previous work, the Pt NPs can be linearly arranged by the surfactant of glucose in lower pH aqueous solution, but we did not observe any welding between the individual NPs for that case and attributed it to a hydrogen bond driven linear self-assembly.[8] With increasing pH value in this work, it is interesting to find that the Pt NPs can be linearly welded and thus a large number of grain boundaries are generated (Figure 1b). A similar phenomenon was also observed in preparing monodisperse Au NPs, and thus, a mesoporous Au NWs network was obtained.[13] The mechanism responsible for the formation of NWs may arise from that the pH could affect the binding and/or redox potential of glucose and thus reduce the effective surface coverage by the individual glucose units. The detailed mechanism needs to be clarified in future work. In summary, the approach to preparing Pt NWs described here is very simple and environmentally benign and also easily scaled up into either mesoporous Pt NW bulk sponges or thin films with a controllable nanopore size.

At any rate, the enchanced CA has been experimentally evidenced in this study by the two model catalytic reactions when the monodisperse Pt near-spherical NPs change into particle-welded NWs. This finding will provide a new idea to improve the CA by creating more grain boundaries on the nanometer scale. This may be done by integrating the monodisperse nanoparticle (or cluster) catalysts into particle-welded nanowires, and thus, it simplifies the cumbersome procedures for handling and separation of the catalysts from the reaction products in continuous operations in industry.

4. Conclusions

A facile, environmentally friendly, and readily scaled-up method has been developed to prepare monodisperse Pt NPs and particle-linked NWs in aqueous solution at room temperature. The results of two catalytic reactions, reduction of either nitrophenol or ferricyanide ions, show that the catalytic activity of monodisperse Pt NPs increases mildly with increasing particle size, whereas Pt NW colloids exhibit a larger CA than the monodisperse Pt NPs with a similar mean size. Although this mechanism of enhanced CA for the Pt NWs remains open, it is expected that the grain boundaries of the Pt NWs, generated when the NPs are linearly linked, might be responsible for the enhanced catalytic activity.

Acknowledgment. This work was supported by the NNSFC (No. 50871028) and the Ministry of Education of China (No. IRT0713). The authors appreciate Dr. Jacob Huang with Kemira Finnchem company for his critical review on this manuscript. X.N.X. appreciates the Northeastern University Research Foundation for Doctor Candidates (No. 200803).

Supporting Information Available: The calculation of surface area of Pt NPs and NWs, TEM images of Pt nanoparticles and nanowires, and UV−vis spectra monitoring the catalytic kinetics are described in the Supporting Information. This material is available free of charge via the Internet at http://pubs.acs.org.

References and Notes

(1) Davis, S. C.; Klabunde, K. J. *Chem. Rev.* **1982**, *82*, 153.
(2) Trudeau, M. L.; Ying, J. Y. *Nanostruct. Mater.* **1996**, *7*, 245.
(3) Vajda, S.; Pellin, M. J.; Greeley, J. P.; Marshall, C. L.; Curtiss, L. A.; Ballentine, G. A.; Elam, J. W.; Catillon-Mucherie, S.; Redfern, P. C.; Mehmood, F.; Zapol, P. *Nat. Mater.* **2009**, *8*, 213.
(4) (a) Narayanan, R.; El-Sayed, M. A. *Nano Lett.* **2004**, *4*, 1343. (b) Narayanan, R.; El-Sayed, M. A. *Langmuir* **2005**, *21*, 2027. (c) Narayanan, R.; Tabor, C.; El-Sayed, M. A. *Top. Catal.* **2008**, *48*, 60. (d) Mahmoud, M. A.; Tabor, C. C.; El-Sayed, M. A.; Ding, Y.; Wang, Z. L. *J. Am. Chem. Soc.* **2008**, *130*, 4590.
(5) Hermanek, M.; Zboril, R.; Medrik, I.; Pechousek, J.; Gregor, C. *J. Am. Chem. Soc.* **2007**, *129*, 10929.
(6) Tian, N.; Zhou, Z.-Y.; Sun, S.-G.; Ding, Y.; Wang, Z. L. *Science* **2007**, *316*, 732.
(7) Lim, B.; Jiang, M.; Camargo, P. H. C.; Cho, E. C.; Tao, J.; Lu, X.; Zhu, Y.; Xia, Y. *Science* **2009**, *324*, 1302.
(8) Liu, J. C.; Raveendran, P.; Qin, G. W.; Ikushima, Y. *Chem. Commun.* **2005**, *23*, 2972.
(9) Liu, J.; Qin, G. W.; Raveendran, P.; Ikushima, Y. *Chem.—Eur. J.* **2006**, *12*, 2131.
(10) Yang, W.; Ma, Y.; Tang, J.; Yang, X. *Colloids Surf., A* **2007**, *302*, 628.
(11) Sharma, R. K.; Sharma, P.; Maitra, A. *J. Colloid Interface Sci.* **2003**, *265*, 134.
(12) Panda, R. K.; Neogi, G.; Ramaswamy, D. *Bull. Soc. Chim. Belg.* **1981**, *90*, 1005.
(13) Qin, G. W.; Liu, J.; Balaji, T.; Xu, X.; Matsunaga, H.; Hakuta, Y.; Zuo, L.; Raveendran, P. *J. Phys. Chem. C* **2008**, *112*, 10352.

JP910864W